Applied Catalysis B: Environmental 343 (2024) 123481

Contents lists available at ScienceDirect

Applied Catalysis B: Environmental

journal homepage: www.elsevier.com/locate/apcatb

Nanozyme-enhanced glucose/O_2 bio-photoelectrochemical system: Taking the challenge of earth diurnal variation

Shuai Hao [a,b], He Zhang [a,*], Xiaoxuan Sun [a,b], Jinxing Chen [a,b], Junfeng Zhai [a], Shaojun Dong [a,b,**]

[a] State Key Laboratory of Electroanalytical Chemistry, Changchun Institute of Applied Chemistry, Chinese Academy of Sciences, Changchun, Jilin 130022, China
[b] University of Science and Technology of China, Hefei, Anhui 230026, China

ARTICLE INFO

Keywords:
Glucose electro-metabolism
High-efficiency biofuels utilization
Photocatalysis
Nanozyme
Renewable resources

ABSTRACT

Achieving efficient and reasonable renewable energy utilization is crucial for sustainable socio-economy development. Herein, an ingenious glucose/O_2 bio-photoelectrochemical system (BPECS) is developed to enhance glucose metabolism process for high-efficiency biofuels utilization. Capturing the intermittent nature of sunlight, glucose metabolism is divided into two-step reasonably. Under dark condition, bio-metabolism catalyzed by glucose oxidase (GOD), is conducted firstly to enrich gluconic acid and H_2O_2. Benefiting from specific electrocatalytic selectivity of $BiVO_4$ photoanode and hemin cathode towards gluconic acid oxidation and H_2O_2 reduction, respectively, electro-matabolism occurs subsequently under light illumination. Moreover, profiting from prominently catalytic stability, a nanozyme-enhanced BPECS is constructed for the first time by integrating GOD-like Au nanoparticles, and a maximum power density of 139.17 μW cm^{-2} with open-circuit voltage of 0.62 V, is obtained. Such a BPECS provides a guiding significance for exploration of renewable energy sources and opens up a new path to expand nanozymes in extensive research fields.

1. Introduction

The rapid growth of population and large-scale expansion of industrialization remarkably accelerate the exhaustion of fossil resources [1], which makes it urgent to exploit renewable resources as alternatives. As the essential component of plant cell wall, cellulose is the most abundant biomass on earth, thus making it significant in sustainable resource treasure house [2–4]. Glucose, the main soluble hydrolysis product of cellulose, can be transformed into value-added chemicals or directly served as renewable fuels in fuel cells (FCs) [5,6]. Among various FCs, enzymatic biofuel cells (EBFCs) use redox enzymes as catalysts to convert chemical energy into electricity directly [7]. As more advanced energy systems, EBFCs have many advantages such as diverse fuel sources, mild operating conditions and good biocompatibility [7,8], which caters to the development of sustainable energy strategy, thus are expected as a next-generation green power device [9]. Nevertheless, in most EBFCs [10–12], glucose oxidases (GODs) or glucose dehydrogenases (GDHs) just convert glucose into gluconic acid to achieve two-electron oxidation, which is far lower than the 24 electrons that can be generated by the complete oxidation of glucose [13,14]. It means that most of energy density will be lost in waste stream, making it dissatisfactory towards high-efficiency energy harnessing. So efficient extraction of chemical energy from glucose into electricity in EBFCs becomes an essential research project. Inspired by natural catabolism, enzyme cascades have been introduced into EBFCs to oxidize glucose completely and harness the energy density of it efficiently by mimicking natural metabolism pathways [9,14]. However, multi-enzyme systems always suffer from incompatibility, difficult immobilization, poor stabilization and high costs [15,16]. For another, photocatalysis was integrated into glucose-powered EBFCs to construct biohybrid photoelectrochemical systems, where the photo-generated charge carriers from photocatalysts transferred to (or from) enzymes [17,18]. This strategy promotes the biocatalytic reactions and makes solar-assisted EBFCs display enhanced catalysis and energy conversion efficiency [19,20]. Nonetheless, efficient connection of enzymes to photoelectrodes and discontinuous energy conversion caused by intermittency of sunlight are still big

* Corresponding author.
** Corresponding author at: State Key Laboratory of Electroanalytical Chemistry, Changchun Institute of Applied Chemistry, Chinese Academy of Sciences, Changchun, Jilin 130022, China.
E-mail addresses: hezhang@ciac.ac.cn (H. Zhang), dongsj@ciac.ac.cn (S. Dong).

https://doi.org/10.1016/j.apcatb.2023.123481
Received 24 August 2023; Received in revised form 2 November 2023; Accepted 6 November 2023
Available online 7 November 2023

obstacles [21]. Herein, developing a new strategy based on the reasonable distribution of solar energy to enhance metabolism process of glucose for high-efficiency biofuels utilization in EBFCs is necessary in the exploitation of sustainable energy.

In this context, we developed a glucose/O_2 bio-photoelectrochemical system (BPECS), consisting of a glucose oxidase (GOD) biocatalyst modified on carbon felt (CF), a bismuth vanadate ($BiVO_4$) photoanode and a hemin cathode, to enhance the glucose metabolism process by adopting a strategy that biocatalysis and photoelectrocatalysis were carried out alternately with the diurnal variation. Under dark condition, two-electron bio-metabolism process of glucose, catalyzed by GOD, was carried out firstly to enrich the metabolin of gluconic acid and H_2O_2. Subsequently, under light illumination, $BiVO_4$ photoanode represented a surprisingly photoelectrocatalytic selectivity towards gluconic acid oxidation, and effective H_2O_2 reduction occurred at the hemin cathode with the same time, so the further electro-metabolism process of glucose was completed successfully (Scheme 1). On basis of this ingenious configuration design, this BPECS can not only enhance the metabolism process of glucose for high-efficiency biofuels utilization, but also generate electricity efficiently and reasonably from both biomass and solar energy. As results, such a GOD-based BPECS exhibited an open-circuit voltage of 0.60 V and a maximum power density of 84.66 μW cm^{-2} (at 0.33 V) under oxygen-saturated condition with 10 mM glucose.

Nevertheless, the long-term stable operation of this GOD-based BPECS is limited by intrinsic drawbacks of natural enzymes, such as poor recyclity, easy denaturation and short active lifetime [12,22]. Recent years, with the intensive study and rapid development of nanotechnology, nanozymes, nanomaterials with intrinsic enzyme-like properties [22,23], have fascinated tremendous research interest. On the one hand, different from the fragility of natural enzymes, nanozymes exhibit remarkably high stability due to their nature of nanomaterials. On the other hand, compared with the high expense and main difficulty of purification for natural enzymes, nanozymes have the appealing advantages of low cost and easy to produce [24,25]. Therefore, nanozymes, the new generation of artificial enzymes [23], are expected as promising alternatives to natural enzymes in practical applications [26]. Among various nanozymes, Au nanoparticles (Au NPs) have been recognized as unique and excellent GOD mimics with privileged biocompatibility. Most importantly, they can catalyze glucose to achieve two-electron oxidation, and produce gluconic acid and H_2O_2 in the presence of oxygen following the similar catalytic pathway of natural GOD [25,27,28], which completely meets the operating requirements of the system we demonstrated. So, we introduced Au NPs into the original BPECS to replace GOD for glucose bio-metabolism to achieve a stable cycling performance with superiority. This new assembled Au NPs-based BPECS highlights the favorable robustness and specific catalysis of nanozyme, and gets rid of its intrinsic drawback of poor selectivity. Our study illustrates that the Au NPs-based BPECS obtains an open-circuit voltage of 0.56 V and a maximum power density of 61.43 μW cm^{-2} (at 0.19 V) under oxygen-saturated condition with 10 mM glucose, slightly lower than the results from GOD-based BPECS. This is mainly due to the catalytic activity of nanozymes is lower than natural enzymes, which is also one of the key problems that existed currently in the development of nanozymes. Therefore, aiming at the construction of a system with higher and more stable output performance, we combine Au NPs with GOD as biocatalyst for glucose bio-metabolism, and this nanozyme-enhanced BPECS exhibits an excellent capacity in electric power harvest with a maximum power density of 139.17 μW cm^{-2} (at 0.27 V) and an open-circuit voltage of 0.62 V. To evaluate the cycling stability of integrated systems, the glucose biofuel is refreshed with the simulation of the diurnal variation. This nanozyme-enhanced BPECS exhibited a superior and reproduceable cycling performance in glucose metabolism compared to GOD-based system. On basis of this integrated configuration design, this BPECS can enhance the glucose metabolism process for high-efficiency biofuels utilization. Furthermore, the introduction of nanozyme improves its cycling stability, thus endowing this developed system with the potential for practical application in the development of large-scale sustainable energy conversion systems based on grid integration.

2. Experimental

The details of the relevant chemicals, catalysts preparation, electrodes fabrication, characterization and measurements involved in the experiments are provided in the Supporting Information.

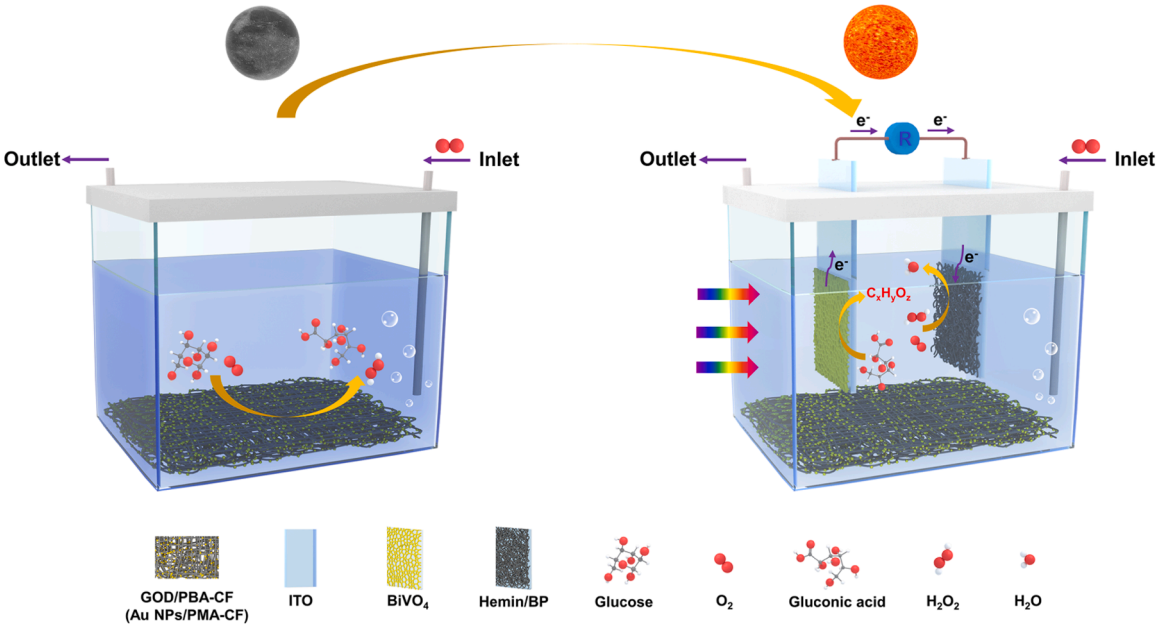

Scheme 1. A diagram of the integrated configuration design and working principle of the glucose/O_2 BPECS.

3. Results and discussion

3.1. Bio-metabolism process of glucose

As a starting point, bio-metabolism process of glucose in BPECS was investigated. As far as known, in the presence of O_2, GOD can catalyze glucose to achieve a two-electron oxidation reaction, and produce H_2O_2 and glucolactone. Then glucolactone is quickly hydrolyzed into gluconic acid in solution. To validate this metabolic pathway, the colorimetric detection of H_2O_2 was evaluated firstly (Fig. 1a). In the colorimetric system, horseradish peroxidase (HRP) was employed to catalyze the oxidation of 3,3′,5,5′-tetramethylbenzidine (TMB), a color indicator, to generate a typical blue product in the presence of H_2O_2. After the incubation of glucose and GOD for 20 min in phosphate buffer solution (PBS, pH 7.0), the characteristic absorbance at 652 nm of TMB_{ox} was clearly observed with the addition of HRP and TMB (Fig. 1b), suggesting the production of H_2O_2 in glucose bio-metabolism process. Then we modified GOD on CF via a biofunctional molecule, 1-pyrenebutyric acid (PBA) that can provide a carboxyl-riched surface to anchor the amino residues of GOD for improving its immobilization, an integrated GOD/PBA-CF biocatalyst was constructed. We employed this GOD/PBA-CF biocatalyst for glucose oxidation overnight and then verified another product, namely gluconic acid, through gas chromatograph-mass spectrometry (GC-MS) analysis. By contrasting with the standard sample, as shown in Fig. 1c, the presence of a relatively strong peak at 16.15 min demonstrates the generation of gluconic acid in this bio-metabolism process and without any other by-products.

3.2. Electro-metabolism process of glucose

Subsequently, the electro-metabolism process of glucose in BPECS was developed. For the oxidation of gluconic acid, we synthesized a $BiVO_4$ photoanode and investigated its photo-electrocatalytic properties. $BiVO_4$, a typical n-type semiconductor, has been widely used for water oxidation in photoelectrochemical water splitting due to its inherent advantages such as substantial light absorption and suitable valence-band edge position [19,29,30]. However, its specific photo-electrocatalytic capacity toward gluconic acid oxidation has been reported rarely. So, in this work, $BiVO_4$ photoanode was developed to achieve gluconic acid oxidation in BPECS. To prepare $BiVO_4$ on indium tin oxide (ITO) substrate, the electrodeposition of BiOI was carried out in a three-electrode electrochemical system firstly, and then this BiOI/ITO was calcined with vanadium precursor for transformation to $BiVO_4$/ITO. To improve its photo-generated charge carriers separation efficiency, the as-prepared $BiVO_4$/ITO was treated by potentiostatic photopolarization to induce oxygen vacancies at surface by applying a potential of 0.8 V (vs. RHE) for 5 h under continuous illumination (Fig. S1) [29], and then the activated $BiVO_4$/ITO photoanode was obtained. To evaluate its surface states, the X-ray photoemission spectrometry (XPS) analysis was adopted. In XPS spectra, the O 1 s spectrum can be fitted into three peaks, including lattice oxygen (O_L), oxygen vacancies (O_V) and chemisorbed oxygen (O_C) [31,32]. The peak intensity of O_V for activated $BiVO_4$/ITO photoanode significantly increased with the ratio from 37.06% to 71.45% compared to pristine $BiVO_4$/ITO, proving that a large amount of oxygen vacancies were induced by potentiostatic photopolarization treatment (Fig. S2). In addition, the strong g signal (g=2.003) in electron paramagnetic resonance (EPR) spectra also proves the increase of O_V on the activated $BiVO_4$/ITO photoanode surface (Fig. S3). Scanning electron microscopy (SEM) images reveal the morphology alteration of photoanode surface (Fig. S4). The pristine $BiVO_4$ film shows a heterogeneous rough surface due to the disordered aggregation of small nanoparticles. After this

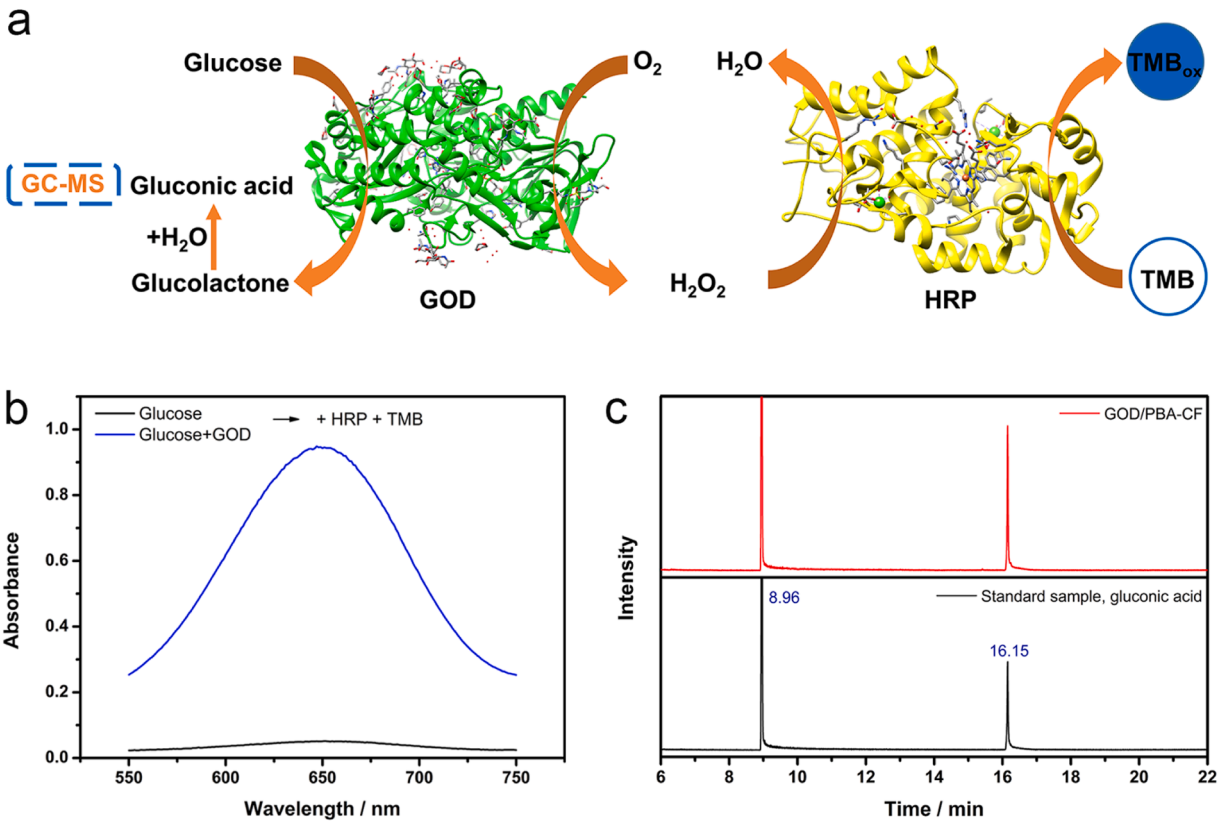

Fig. 1. Validation of the metabolin in glucose bio-metabolism process catalyzed by GOD. (a) Schematic illustration of metabolin detection. (b) Absorption spectra of different samples for colorimetric detection of H_2O_2. (c) GC-MS analysis of different samples for detection of gluconic acid. The peaks at 16.15 and 8.96 min are assigned to gluconic acid and phosphate, respectively.

treatment, a smoother film surface with homogeneous nanoworm-like agglomerates is exposed. The X-ray diffraction (XRD) pattern of the activated photoanode exhibits the monoclinic $BiVO_4$ phase (JCPDS No. 14–0688), and all diffraction peaks have no significant change compared to pristine $BiVO_4$ (Fig. S5), suggesting that the crystalline phase remains stable during this treatment. To evaluate the photoelectrocatalytic performance of $BiVO_4$/ITO photoanode toward gluconic acid oxidation, linear sweep voltammetry (LSV) experiments were conducted. As shown in Fig. 2a, under light illumination (AM 1.5 G), the pristine $BiVO_4$/ITO electrode exhibits an anodic photocurrent density of 0.68 mA cm^{-2} at 0.3 V (vs. Ag/AgCl) in the presence of 20 mM gluconic acid, with an onset potential about - 0.30 V. After the potentiostatic photopolarization treatment, the photocatalytic current of activated $BiVO_4$/ITO photoanode enhances remarkably and reaches 2.20 mA cm^{-2} at 0.30 V shown in Fig. 2b, which is 2.2 times higher than that of the pristine $BiVO_4$/ITO electrode. This significantly enhanced photocatalytic activity is attributed to the increasement of oxygen vacancies at photoanode/electrolyte interface, which can effectively promote charges transfer and reduce surface recombination, further improving the anodic kinetics of gluconic acid oxidation. Therefore, the activated $BiVO_4$/ITO photoanode was employed as the final photoanode for all subsequent experiments. In the control experiment, the $BiVO_4$/ITO photoanode displays a weak catalytic current for direct photoelectrochemical oxidation of glucose compared with gluconic acid (Fig. S6), suggesting that such a photoanode represents a highly photoelectrocatalytic selectivity toward gluconic acid oxidation. This surprising electrochemical phenomenon might be ascribed to the intrinsic electrocatalytic selectivity of $BiVO_4$ towards gluconic acid oxidation. Under dark condition, the low onset potential of about 0.2 V (vs. RHE) can be observed for the electrocatalytic oxidation of gluconic acid on $BiVO_4$/ITO photoanode surface, and the catalytic current densities significantly increase with gluconic acid concentrations (Fig. S7). The above results indicate that the thermodynamic energy barrier of this reaction is quite low, so the gluconic acid oxidation is more favorable on $BiVO_4$ surface compared with water and/or glucose [33]. In BPECS, this specific catalytic characteristic of $BiVO_4$/ITO photoanode plays a crucial role in multi-step metabolism of glucose. Furthermore, in order to evaluate the by-products of gluconic acid oxidation on $BiVO_4$/ITO photoanode, a long-term photoelectrochemical reaction (at a constant potential of 0.2 V) was carried out in a typical H-type cell. The reactive anolyte was taken out per 12 h for GC-MS analysis. By contrasting with the standard samples, the main product of anodic reaction is arabinose ($C_5H_{10}O_5$), which is also a value-added aldopentose in bio-refinery process (Fig. S8) [34].

For the effective reduction of H_2O_2, a hemin (iron protoporphyrin) cathode was fabricated and its electrochemical performance was

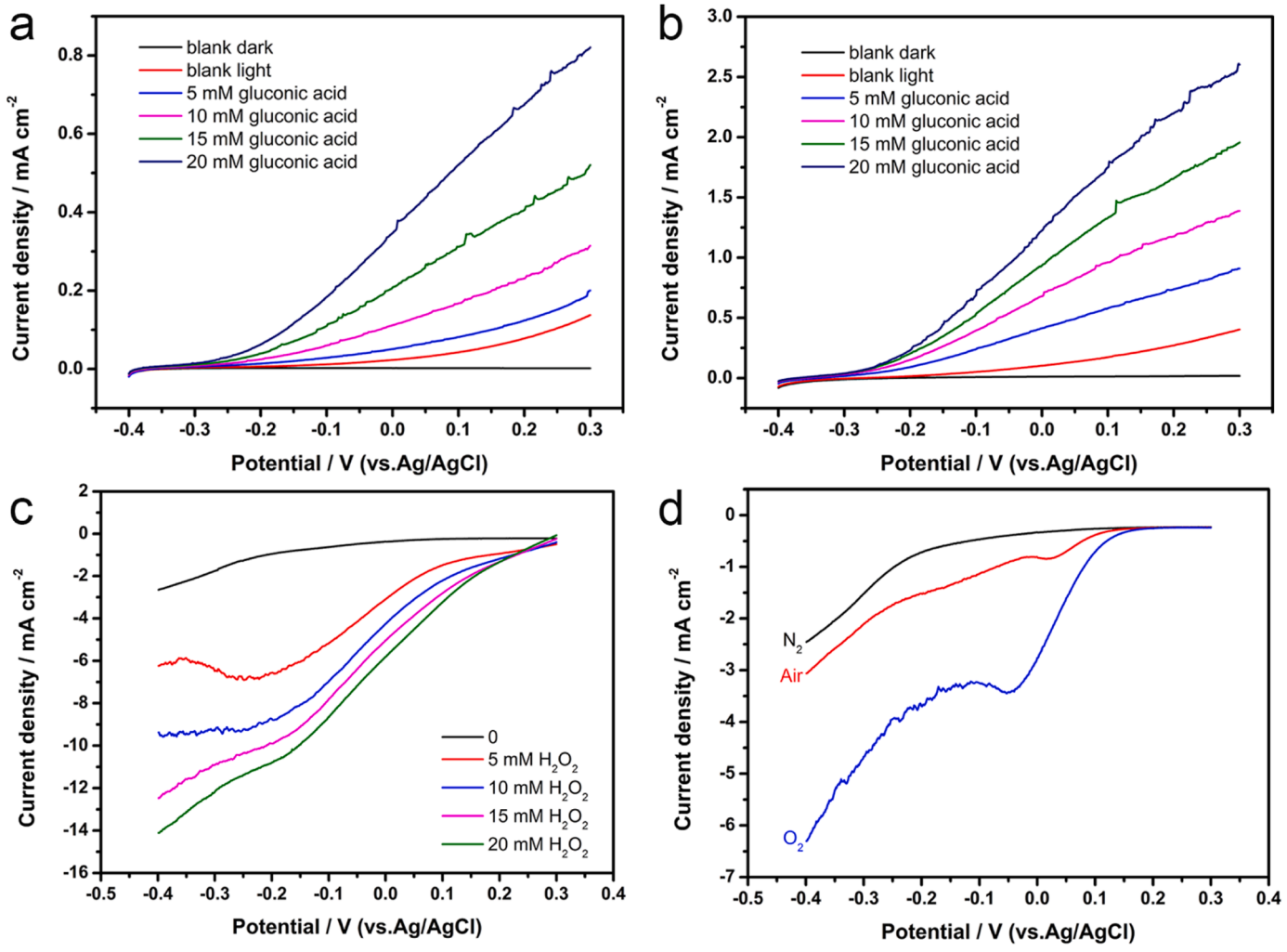

Fig. 2. Electrochemical performance of $BiVO_4$/ITO photoanode and hemin/BP cathode. (a, b) LSV curves of pristine $BiVO_4$/ITO (a) and activated $BiVO_4$/ITO photoanode (b) in 0.1 M PBS (pH 7.0) containing different concentrations of gluconic acid under light illumination (AM 1.5 G). (c, d) LSV curves of hemin/BP cathode in 0.1 M PBS (pH 7.0) (c) containing different concentrations of H_2O_2 under nitrogen-saturated condition and (d) saturated with nitrogen, air or oxygen, respectively. Scan rate: 10 mV s^{-1}.

discussed. Benefitting from the large specific surface areas, high conductivity and biocompatibility [35,36], buckypaper (BP), a carbon nanotubes-based substrate material with a large number of interconnected pores (Fig. S9), was employed to support hemin for constructing the cathode. Meanwhile, an amino-riched biofunctional molecule, 1-pyrenemethylamine hydrochloride (PMA), was introduced to stabilize the immobilization of hemin on BP by π-π stacking and electrostatic interaction. In XPS analysis of hemin/PMA/BP, the peaks at 399.7 eV and 398.5 eV in N 1 s spectrum are assigned to the nitrogen atoms in amino group of PMA and pyrrole of hemin, respectively, implying the successful modification of PMA and hemin on BP surface (Fig. S10f) [37]. In addition, the inductively coupled plasma (ICP) spectrometry results suggest that the content of Fe increases markedly of hemin/BP compared to BP, further proving the immobilization of hemin (Table S1). To evaluate the electrochemical performance of this hemin/BP cathode toward H_2O_2 reduction, we carried out LSV analysis in nitrogen-saturated 0.1 M PBS (pH 7.0). As shown in Fig. 2c, the hemin/BP cathode shows remarkably catalytic activity toward H_2O_2 reduction and the cathodic current reaches 10.42 mA cm^{-2} at - 0.30 V (vs.Ag/AgCl) in the presence of 20 mM H_2O_2, with an onset potential about 0.30 V. Furthermore, it is noteworthy that the hemin/BP cathode also exhibits electrocatalytic activity for oxygen reduction reaction (ORR). The reduction current densities of hemin/BP cathode reach 0.59 and 3.15 mA cm^{-2} at - 0.30 V (vs.Ag/AgCl) under air- and oxygen-saturated conditions, respectively, and an onset potential about 0.20 V is obtained for ORR (Fig. 2d). This result indicates that the dissolved oxygen can be served as a supplement to complete the cathode reaction when H_2O_2, generated from glucose bio-metabolism, is exhausted. This double-response electrochemical performance of hemin/BP makes electro-metabolism process of glucose not limited by cathode, which implies that the reaction of gluconic acid oxidation at $BiVO_4$/ITO photoanode can be effectively carried out, so the electro-metabolism of glucose will be achieved in this fabricated photo-biofuel cell (PBFC). Furthermore, considering the construction of a single-chamber system, the interference assays were also analyzed. The reduction currents of hemin/BP cathode for H_2O_2 and O_2 have slight changes after the addition of glucose or gluconic acid in control experiments (Fig. S11), indicating that electrocatalytic behaviors of cathode cannot be interfered in the presence of glucose and/or gluconic acid. To test the electrochemical performance of this fabricated one-chamber PBFC, LSV experiments were conducted under different conditions (Fig. S12 and Table S2). When the $BiVO_4$/ITO photoanode was fed with 20 mM gluconic acid, hemin/BP cathode was fed with 20 mM H_2O_2, the PBFC obtained a maximum power output density of 0.36 mW cm^{-2} at 0.29 V with an open-circuit voltage of 0.57 V under nitrogen-saturated condition (Fig. S12a). We also employed ORR as the main reaction for hemin/BP cathode, the PBFC exhibited a maximum power output density of 0.15 mW cm^{-2} at 0.20 V under oxygen-saturated condition (Fig. S12b). The exceptional electrochemical performance of this PBFC demonstrates that it possesses operating feasibility and outstanding

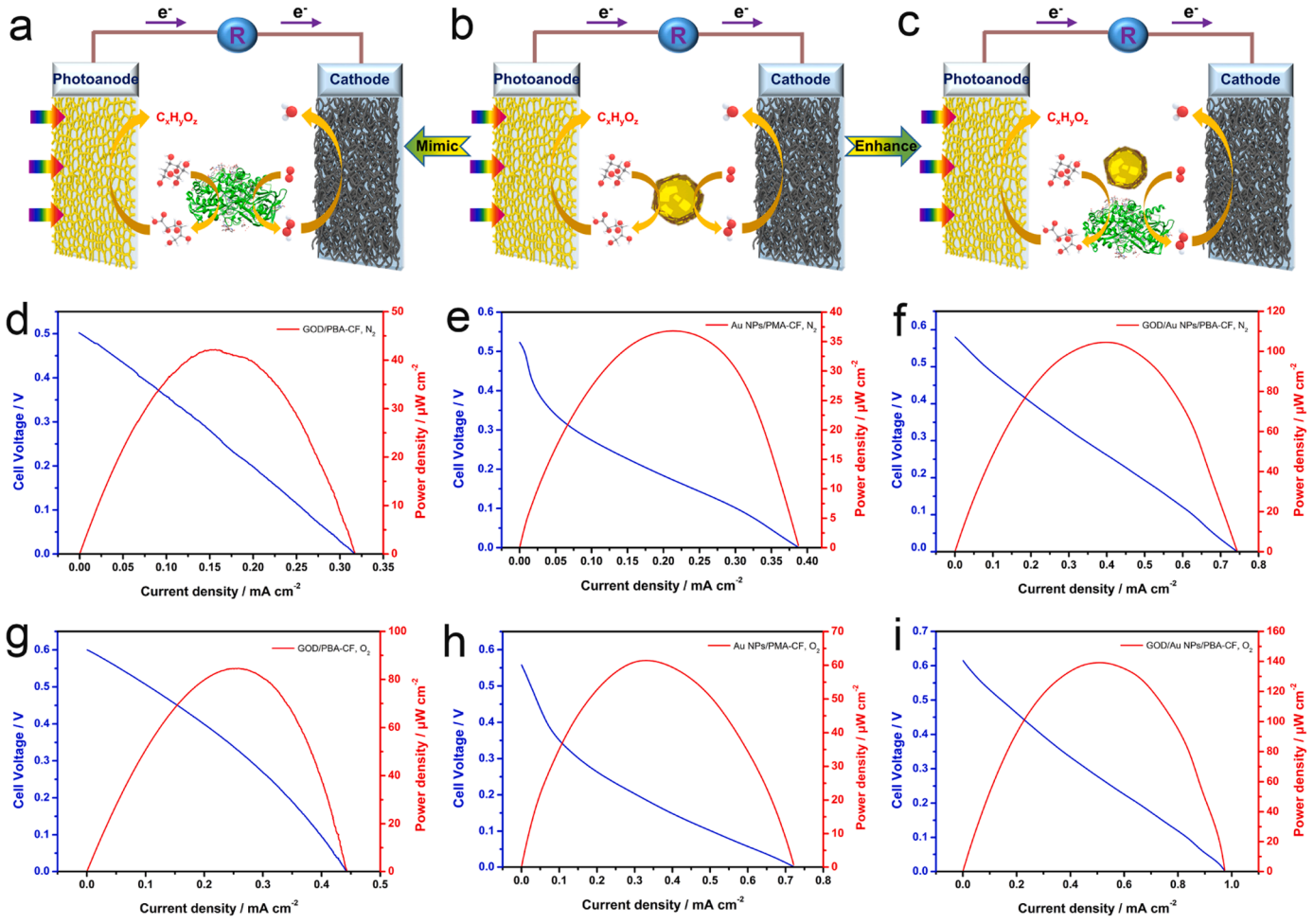

Fig. 3. Working principle and electrochemical performance of glucose/O_2 BPECS. (a, b, c) Diagrams of GOD-based (a), Au NPs-based (b) and GOD/Au NPs-based BPECS (c). (d-i) LSV curves of PBFC and the corresponding power densities measured in nitrogen- (d, e, f) and oxygen- (g, h, i) saturated conditions under light illumination (AM 1.5 G), collected after bio-metabolism of 10 mM glucose catalyzed by GOD/PBA-CF (d, g), Au NPs/PMA-CF (e, h) and GOD/Au NPs/ PBA-CF (f, i) for 12 h in oxygen-saturated 0.1 M PBS (pH 7.0) under dark condition. Scan rate: 1 mV s^{-1}.

potential as a unit component of BPECS.

3.3. Electrochemical performance of developed BPECSs

Benefitting from the excellent performance of the above individual components, a single-chamber BPECS was developed by integrating the GOD/PBA-CF biocatalyst with PBFC to achieve glucose multi-step metabolism (Fig. 3a and **S13**), and then its working principle and electrochemical performance were studied. Based on the intermittent nature of sunlight, the glucose metabolism process can be divided into two-step in this BPECS. Firstly, bio-metabolism process of glucose, catalyzed by GOD/PBA-CF biocatalyst, was carried out to enrich the gluconic acid and H_2O_2 in the presence of O_2 through an incubation for 12 h under dark condition (Fig. S13a). Subsequently, we arranged the $BiVO_4$/ITO photoanode and hemin/BP cathode into this BPECS opposite each other (Fig. S13b, c). Under light illumination, the $BiVO_4$ photoanode generated electrons and holes, the photo-generated holes were employed for gluconic acid oxidation at the photoanode surface, while the photo-generated electrons were transferred to hemin/BP cathode through an external circuit to reduce H_2O_2 to H_2O, so the electro-metabolism process was completed. Considering the electrocatalytic capability of hemin/BP cathode for ORR besides H_2O_2, we carried out LSV experiments under nitrogen- and oxygen-saturated conditions for comparison to evaluate the electrochemical performance of BPECS. As results, this GOD-based BPECS obtains a maximum power output density of 84.66 μW cm^{-2} at 0.33 V and 42.17 μW cm^{-2} at 0.27 V under oxygen- and nitrogen-saturated conditions, respectively, and open-circuit voltages of 0.60 V and 0.50 V are observed correspondingly (Fig. 3g, d). In control group (catalyst-free, Fig. S14a), a power density of 15.16 μW cm^{-2} at 0.17 V is obtained, which is ascribed to the fact that glucose oxidation and oxygen reduction occur at $BiVO_4$/ITO photoanode and hemin/BP cathode, respectively. These results demonstrate that the developed BPECS not only achieves multi-step oxidation of glucose biofuels for improving its metabolism process, but also converts electric power efficiently and reasonably from both biomass and solar energy.

Nevertheless, the development of enzyme-based electrochemical systems in practical application is dramatically hindered by inherent fragility of natural enzymes, due to the easy denaturation and inactivation of enzymatic protein under harsh reaction conditions, such as high temperature, extreme pH and organic solvents [38]. To break this limitation, tremendous efforts have been devoted in various research fields. On the one hand, the directed evolution of natural enzymes has been engineered for improving their adaptability to deal with the complex abiotic environments [39]. On the other hand, artificial enzyme mimics were developed to replace natural enzymes in different catalytic systems due to their superior robustness and low cost. With the intensive study of nanomaterials, nanozymes, the new generation of artificial enzymes, have attracted a lot of attention for their appealing characteristics, such as high stability, tunable activity and easy to produce [24, 25]. Therefore, we employed nanozyme as a promising alternative for natural enzyme to enhance the operating stability of our developed system. Specifically, Au NPs, the GOD-like nanozymes, were introduced into the original BPECS to replace GOD for glucose bio-metabolism process. Firstly, polyacrylic acid (PAA)-stabilized Au NPs were prepared in aqueous solution according to a recently reported method in our lab [40]. Transmission electron microscopy (TEM) image revealed that the uniformly sized Au NPs with average diameters of about 1.2–1.7 nm were obtained (Fig. S15). Due to such small size of nanoparticles and the low steric hindrance of PAA, the as-prepared PAA-Au NPs exhibit excellent catalytic capacity for glucose oxidation [40]. In order to investigate its GOD-like catalytic activity, the steady-state kinetics were analyzed by Michaelis-Menten equation ($v=v_{max}\cdot[s]/(K_m+[s])$). The Michaelis-Menten curve was obtained by varying the concentrations of glucose substrate ([s]), and the Michaelis constant (K_m) and maximum reaction velocity (v_{max}) were fitted to be 21.75 mM and 0.34 μM s^{-1}, respectively (Fig. S16). The K_m of PAA-Au NPs is quite higher than that of GOD (4.87 mM) [41], indicating that the affinity of Au NPs to glucose substrate is worse than natural enzyme. We used the as-prepared Au NPs to catalyze glucose oxidation and verified the metabolin. The same colorimetric detection method was carried out in Au NPs-based catalytic system again, the absorption peak at 622 nm appeared after the addition of HRP and TMB, which proved the generation of H_2O_2 in this mimic bio-metabolism process (Fig. S17). It is worth mentioning that the characteristic absorption peak of TMB_{ox} shifts negatively from 652 nm to 622 nm, it could be ascribed to the electrostatic interaction between PAA and positively charged TMB_{ox} leads to the formation of indigo complex [42]. For constructing the Au NPs-based catalyst, an in-situ growing strategy was employed to integrate Au NPs onto a PMA modified CF, and then the Au NPs/PMA-CF catalyst was obtained (see Experimental Section in Supporting Information for details). We used this Au NPs/PMA-CF catalyst for glucose oxidation overnight, and the peak at 16.15 min in GC-MS analysis confirmed that gluconic acid is the only one product in glucose bio-metabolism process (Fig. S18). These results demonstrate that Au NPs follow the similar catalytic pathway of natural GOD, which completely meets the operating requirements of the original system. Therefore, we replaced the GOD/PBA-CF biocatalyst with Au NPs/PMA-CF for glucose bio-metabolism and integrated it with PBFC to develop an Au NPs-based BPECS (Fig. 3b). The elecrochemical analysis reveals that this new assembled system obtains a maximum power output density of 61.43 μW cm^{-2} at 0.19 V and 36.81 μW cm^{-2} at 0.17 V under oxygen- and nitrogen-saturated conditions with 10 mM glucose, respectively, and open-circuit voltages of 0.56 V and 0.52 V are observed correspondingly (Fig. 3h, e), demonstrating the multi-step metabolism process of glucose is achieved successfully in this assembled Au NPs-based BPECS. Nevertheless, its maximum power output density is slightly lower than that of GOD-based BPECS, due to the catalytic activity of Au NPs is lower than that of natural GOD, which is consistent with the results from steady-state kinetic analysis. Given that the high catalytic activity of natural enzymes and the outstanding catalytic stability of nanozymes, we combined GOD and Au NPs as the catalyst for glucose bio-metabolism and integrated it with PBFC to construct a nanozyme-enhanced BPECS (Fig. 3c). Due to the stabilizer PAA on the surface of Au NPs possesses a large amount of carboxyl groups, which is more conducive for the further immobilization of GOD, therefore, GOD/Au NPs/PBA-CF, a high-efficiency biocatalyst was obtained. When integrating it with $BiVO_4$/ITO photoanode and hemin/BP cathode, the new developed system yields maximum power output densities of 139.17 μW cm^{-2} at 0.27 V and 104.51 μW cm^{-2} at 0.26 V under oxygen- and nitrogen-saturated conditions with 10 mM glucose, respectively, and open-circuit voltages of 0.62 V and 0.58 V are observed correspondingly (Fig. 3i, f). The results in terms of open-circuit voltage and maximum power output density are superior to the relevant glucose biofuel cells (or photo-biofuel cells) in previously reported studies (shown in Table S3). The above discussion suggests that a nanozyme-enhanced BPECS with exceptional electrochemical performance was successfully constructed.

3.4. Long-term cycling stability of developed BPECSs

Finally, long-term cycling stability of this developed BPECS was evaluated. As shown in Fig. 4a, bio-metabolism and electro-metabolism process were carried out alternately in BPECS by refreshing the glucose biofuels with the simulation of the diurnal variation, and the voltage of PBFC was monitored at a constant discharge current density of 50 μA cm^{-2}. As shown in Fig. 4b, in GOD-based BPECS, the voltage of PBFC has an obvious fluctuation during five cycles and exhibits a significant decrease tendency, which is mainly ascribed to the poor recyclability of natural enzymes. Conversely, as for Au NPs-based BPECS, the voltage of PBFC remains steady in five consecutive cycles (Fig. 4d), revealing that an exceptionally stable and reproduceable cycling performance is achieved in glucose metabolism. This is attributed to the remarkably high

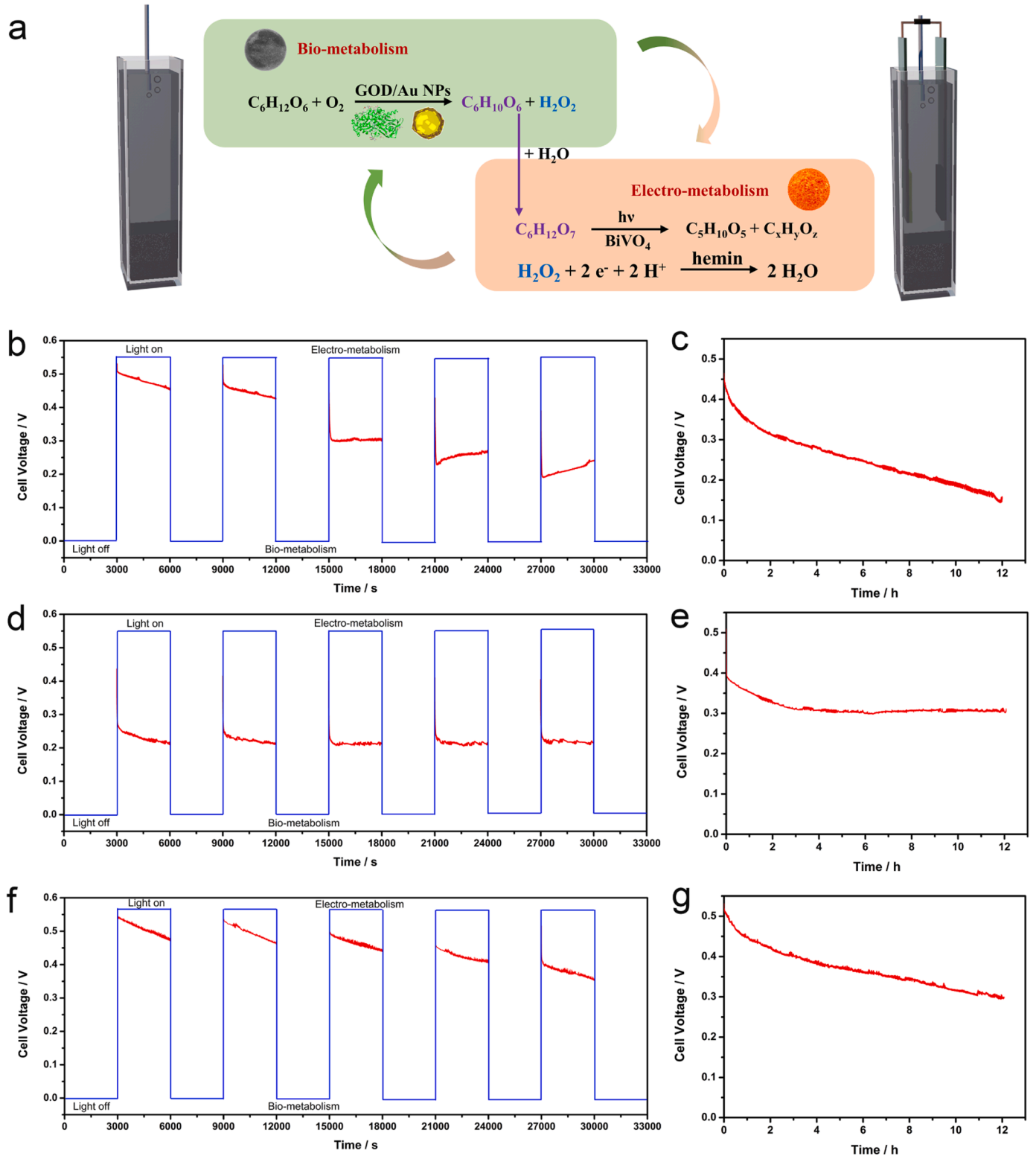

Fig. 4. The schematic illustration of long-term cycling stability measurement (a) for GOD-based (b, c), Au NPs-based (d, e) and GOD/Au NPs-based (f, g) BPECS. The chronopotentiometric (E-t) curves of electro-metabolism process measured at 50 μA cm^{-2} in oxygen-saturated condition under light illumination (AM 1.5 G), collected after bio-metabolism process of 10 mM glucose in oxygen-saturated 0.1 M PBS (pH 7.0) for 3000 s (b, d, f) and 12 h (c, e, g) under dark condition.

catalytic stability of Au NPs, implying that the introduction of nanozyme endows the system with potential for practical application due to the exclusion of biotic components. As far as we know, this is the first example, in the true sense, to achieve the successful replacement from natural enzymes to nanozymes in enzyme-based electrochemical systems, which carries a significant breakthrough for the practical application of nanozymes. Nevertheless, the cell voltage of Au NPs-based BPECS is smaller than that of GOD-based system, which is due to the lower catalytic activity of Au NPs compared with GOD, resulting in less accumulation of gluconic acid and H_2O_2 after bio-metabolism in

such a short period of time. To compensate the shortages of above two systems mentioned, we have constructed a nanozyme-enhanced system and evaluated its cycling performance. In GOD/Au NPs-based BPECS (Fig. 4f), the cell voltage of PBFC is maintained at around 0.5 V with a more gentle decrease within five consecutive cycles compared with GOD-based system, indicating that the integration of nanozyme enhances the cycling stability of original system. To demonstrate the operating capacity of the assembled systems with diurnal variation effectively, we prolong the reaction time of biocatalysis and photoelectrocatalysis, namely, one night (12 h) for bio-metabolism and one day (12 h) for electro-metabolism. The voltage of GOD-based BPECS decreases rapidly during entire electro-metabolism process (Fig. 4c), while that for Au NPs-based system is quite stable after 2 h (Fig. 4e). This is mainly owing to the bio-metabolism process of GOD-based BPECS collects a large quantity of H_2O_2 over a short period. On the one hand, high concentrations of H_2O_2 inhibit the catalytic activity of GOD, and on the other hand, the gradual decomposition of H_2O_2 leads to a decrease in cathode current density. On the contrary, the Au NPs-based bio-metabolism process can generate H_2O_2 slowly and stably, providing a continuous and steady supply for cathode. Subsequently, we assessed the GOD/Au NPs-based system (Fig. 4g), this new assembled nanozyme-enhanced BPECS achieved higher cell voltage and relatively stable discharge performance in electro-metabolism process compared with GOD-based BPECS. These results indicate that the developed BPECSs can enhance the glucose metabolism process for high-efficiency biofuels utilization, and what's more, the introduction of nanozyme improves the long-term cycling stability of the system to take the challenge of earth diurnal variation.

4. Conclusions

In summary, integrating a PBFC, that consists a $BiVO_4$ photoanode and a hemin cathode, with GOD-based biocatalyst, an ingeniously designed glucose/O_2 BPECS was developed to achieve multi-step metabolism of glucose biofuels. Capturing the intermittent nature of sunlight, the glucose metabolism was divided into two-step reasonably in BPECS. Under dark condition, the bio-matebolism process of glucose, catalyzed by GOD-based biocatalyst, was carried out firstly to enrich gluconic acid and H_2O_2. Subsequently, benefiting from the superior photo-/electrocatalytic performance of $BiVO_4$ photoanode and hemin cathode towards gluconic acid oxidation and H_2O_2 reduction, respectively, further electro-metabolism process of glucose was completed under light illumination. Based on this strategy, the integrated BPECS not only enhances the glucose metabolism process for high-efficiency biofuels utilization, but also achieves multiple energy conversion (i. e., biomass-to-electric and solar-to-electric energy conversions). As a result, a maximum power density of 84.66 μW cm^{-2}, with an open-circuit voltage of 0.60 V, was obtained. Considering the inherent fragility of natural enzymes, furthermore, an Au NPs-based BPECS was constructed by replacing GOD with Au NPs for glucose bio-metabolism, and exhibited an exceptionally stable and reproduceable long-term cycling performance. This Au NPs-based BPECS not only highlights the superior stability and specific catalysis of nanozyme, but also provides a non-selective catalytic scenario for nanozyme application. In response to the advantages of natural enzymes in catalytic activity and nanozymes in catalytic stability, we combined GOD and Au NPs as the catalyst for glucose bio-metabolism, and this nanozyme-enhanced BPECS exhibited excellent electrochemical performance and long-term cycling stability. Overall, such an ingenious glucose/O_2 BPECS provides a new strategy for high-efficiency biofuels utilization, and the integration of nanozymes carries a bright prospect for its practical application in the efficient and reasonable exploitation of renewable energy sources.

CRediT authorship contribution statement

Shuai Hao: Conceptualization, Methodology, Investigation, Data curation, Writing - original draft; **He Zhang:** Conceptualization, Formal analysis, Validation; **Xiaoxuan Sun**: Investigation, Discussion; **Jinxing Chen:** Investigation, Discussion; **Junfeng Zhai:** Investigation, Discussion; **Shaojun Dong:** Writing - review & editing, Supervision, Project administration, Funding acquisition.

Declaration of Competing Interest

The authors declare that they have no known competing financial interests or personal relationships that could have appeared to influence the work reported in this paper.

Data Availability

Data will be made available on request.

Acknowledgement

This work was financially supported by the National Natural Science Foundation of China (Nos. 22274146 and 22074137).

Appendix A. Supporting information

Supplementary data associated with this article can be found in the online version at doi:10.1016/j.apcatb.2023.123481.

References

[1] H. Lu, J. Tournet, K. Dastafkan, Y. Liu, Y.H. Ng, S.K. Karuturi, C. Zhao, Z. Yin, Noble-metal-free multicomponent nanointegration for sustainable energy conversion, Chem. Rev. 121 (2021) 10271–10366, https://doi.org/10.1021/acs.chemrev.0c01328.
[2] P. Purushotham, R.Y. Ho, J. Zimmer, Architecture of a catalytically active homotrimeric plant cellulose synthase complex, Science 369 (2020) 1089–1094, https://doi.org/10.1126/science.abb2978.
[3] D. Ye, S. Rongpipi, S.N. Kiemle, W.J. Barnes, A.M. Chaves, C. Zhu, V.A. Norman, A. Liebman-Pelaez, A. Hexemer, M.F. Toney, A.W. Roberts, C.T. Anderson, D. J. Cosgrove, E.W. Gomez, E.D. Gomez, Preferred crystallographic orientation of cellulose in plant primary cell walls, Nat. Commun. 11 (2020), 4720, https://doi.org/10.1038/s41467-020-18449-x.
[4] F. Hammerer, L. Loots, J.L. Do, J.P.D. Therien, C.W. Nickels, T. Friscic, K. Auclair, Solvent-free enzyme activity: quick, high-yielding mechanoenzymatic hydrolysis of cellulose into glucose, Angew. Chem., Int. Ed. 57 (2018) 2621–2624, https://doi.org/10.1002/anie.201711643.
[5] O.L. Li, R. Ikura, T. Ishizaki, Hydrolysis of cellulose to glucose over carbon catalysts sulfonated via a plasma process in dilute acids, Green. Chem. 19 (2017) 4774–4777, https://doi.org/10.1039/c7gc02143g.
[6] L. Hu, L. Lin, Z. Wu, S. Zhou, S. Liu, Chemocatalytic hydrolysis of cellulose into glucose over solid acid catalysts, Appl. Catal. B-Environ. 174–175 (2015) 225–243, https://doi.org/10.1016/j.apcatb.2015.03.003.
[7] X. Xiao, H.Q. Xia, R. Wu, L. Bai, L. Yan, E. Magner, S. Cosnier, E. Lojou, Z. Zhu, A. Liu, Tackling the challenges of enzymatic (Bio)fuel cells, Chem. Rev. 119 (2019) 9509–9558, https://doi.org/10.1021/acs.chemrev.9b00115.
[8] Y. Chen, W. Ji, K. Yan, J. Gao, J. Zhang, Fuel cell-based self-powered electrochemical sensors for biochemical detection, Nano Energy 61 (2019) 173–193, https://doi.org/10.1016/j.nanoen.2019.04.056.
[9] Z. Zhu, Y.P. Zhang, In vitro metabolic engineering of bioelectricity generation by the complete oxidation of glucose, Metab. Eng. 39 (2017) 110–116, https://doi.org/10.1016/j.ymben.2016.11.002.
[10] J.L. Hammond, A.J. Gross, F. Giroud, C. Travelet, R. Borsali, S. Cosnier, Solubilized enzymatic fuel cell (SEFC) for quasi-continuous operation exploiting carbohydrate block copolymer glyconanoparticle mediators, ACS Energy Lett. 4 (2019) 142–148, https://doi.org/10.1021/acsenergylett.8b01972.
[11] C.H. Kwon, Y. Ko, D. Shin, S.W. Lee, J. Cho, Highly conductive electrocatalytic gold nanoparticle-assembled carbon fiber electrode for high-performance glucose-based biofuel cells, J. Mater. Chem. A 7 (2019) 13495–13505, https://doi.org/10.1039/c8ta12342j.
[12] H. Zhang, L. Huang, J. Chen, L. Liu, X. Zhu, W. Wu, S. Dong, Bionic design of cytochrome c oxidase-like single-atom nanozymes for oxygen reduction reaction in enzymatic biofuel cells, Nano Energy 83 (2021), 105798, https://doi.org/10.1016/j.nanoen.2021.105798.
[13] Z. Zhu, C. Ma, Y.H. Percival Zhang, Co-utilization of mixed sugars in an enzymatic fuel cell based on an in vitro enzymatic pathway, Electrochim. Acta 263 (2018) 184–191, https://doi.org/10.1016/j.electacta.2017.11.083.
[14] S. Xu, S.D. Minteer, Enzymatic biofuel cell for oxidation of glucose to CO_2, ACS Catal. 2 (2012) 91–94, https://doi.org/10.1021/cs200523s.

[15] S. Fan, B. Liang, X. Xiao, L. Bai, X. Tang, E. Lojou, S. Cosnier, A. Liu, Controllable display of sequential enzymes on yeast surface with enhanced biocatalytic activity toward efficient enzymatic biofuel cells, J. Am. Chem. Soc. 142 (2020) 3222–3230, https://doi.org/10.1021/jacs.9b13289.
[16] Z. Sun, Q. Zhao, R. Haag, C. Wu, Responsive emulsions for sequential multienzyme cascades, Angew. Chem., Int. Ed. 60 (2021) 8410–8414, https://doi.org/10.1002/anie.202013737.
[17] M. Riedel, S. Hofs, A. Ruff, W. Schuhmann, F. Lisdat, A tandem solar biofuel cell: harnessing energy from light and biofuels, Angew. Chem., Int. Ed. 60 (2021) 2078–2083, https://doi.org/10.1002/anie.202012089.
[18] J. Kim, C.B. Park, Shedding light on biocatalysis: photoelectrochemical platforms for solar-driven biotransformation, Curr. Opin. Chem. Biol. 49 (2019) 122–129, https://doi.org/10.1016/j.cbpa.2018.12.002.
[19] D.S. Choi, J. Kim, F. Hollmann, C.B. Park, Solar-assisted ebiorefinery: photoelectrochemical pairing of oxyfunctionalization and hydrogenation reactions, Angew. Chem., Int. Ed. 59 (2020) 15886–15890, https://doi.org/10.1002/anie.202006893.
[20] N. Yang, Y. Tian, M. Zhang, X. Peng, F. Li, J. Li, Y. Li, B. Fan, F. Wang, H. Song, Photocatalyst-enzyme hybrid systems for light-driven biotransformation, Biotechnol. Adv. 54 (2022), 107808, https://doi.org/10.1016/j.biotechadv.2021.107808.
[21] H. Zhang, L. Huang, J. Zhai, S. Dong, Water/oxygen circulation-based biophotoelectrochemical system for solar energy storage and release, J. Am. Chem. Soc. 141 (2019) 16416–16421, https://doi.org/10.1021/jacs.9b08046.
[22] J. Chen, Q. Ma, M. Li, D. Chao, L. Huang, W. Wu, Y. Fang, S. Dong, Glucose-oxidase like catalytic mechanism of noble metal nanozymes, Nat. Commun. 12 (2021), 3375, https://doi.org/10.1038/s41467-021-23737-1.
[23] H. Wei, E. Wang, Nanomaterials with enzyme-like characteristics (nanozymes): next-generation artificial enzymes, Chem. Soc. Rev. 42 (2013) 6060–6093, https://doi.org/10.1039/c3cs35486e.
[24] L. Huang, J.X. Chen, L.F. Gan, J. Wang, S.J. Dong, Single-atom nanozymes, Sci. Adv. 5 (2019), eaav5490, https://doi.org/10.1126/sciadv.aav5490.
[25] W. Wu, L. Huang, E. Wang, S. Dong, Atomic engineering of single-atom nanozymes for enzyme-like catalysis, Chem. Sci. 11 (2020) 9741–9756, https://doi.org/10.1039/d0sc03522j.
[26] H. Wang, K. Wan, X. Shi, Recent advances in nanozyme research, Adv. Mater. 31 (2019), 1805368, https://doi.org/10.1002/adma.201805368.
[27] J. Chen, W. Wu, L. Huang, Q. Ma, S. Dong, Self-indicative gold nanozyme for H_2O_2 and glucose sensing, Chem. -Eur. J. 25 (2019) 11940–11944, https://doi.org/10.1002/chem.201902288.
[28] L. Fan, D. Lou, H. Wu, X. Zhang, Y. Zhu, N. Gu, Y. Zhang, A novel AuNP-based glucose oxidase mimic with enhanced activity and selectivity constructed by molecular imprinting and O_2-containing nanoemulsion embedding, Adv. Mater. Interfaces 5 (2018), 1801070, https://doi.org/10.1002/admi.201801070.
[29] R.T. Gao, L. Wang, Stable cocatalyst-Free $BiVO_4$ photoanodes with passivated surface states for photocorrosion inhibition, Angew. Chem., Int. Ed. 59 (2020) 23094–23099, https://doi.org/10.1002/anie.202010908.
[30] H. Zhang, Y. Yu, L. Zhang, S. Dong, Fuel-free bio-photoelectrochemical cells based on a water/oxygen circulation system with a Ni:FeOOH/$BiVO_4$ photoanode, Angew. Chem., Int. Ed. 57 (2018) 1547–1551, https://doi.org/10.1002/anie.201710738.
[31] S. Jin, X. Ma, J. Pan, C. Zhu, S.E. Saji, J. Hu, X. Xu, L. Sun, Z. Yin, Oxygen vacancies activating surface reactivity to favor charge separation and transfer in nanoporous $BiVO_4$ photoanodes, Appl. Catal. B-Environ. 281 (2021), 119477, https://doi.org/10.1016/j.apcatb.2020.119477.
[32] S. Feng, T. Wang, B. Liu, C. Hu, L. Li, Z.J. Zhao, J. Gong, Enriched surface oxygen vacancies of photoanodes by photoetching with enhanced charge separation, Angew. Chem., Int. Ed. 59 (2020) 2044–2048, https://doi.org/10.1002/anie.201913295.
[33] H. Zhang, X. Sun, S. Hao, S. Dong, A solar-rechargeable bio-photoelectrochemical system based on carbon tracking strategy for enhancement of glucose electrometabolism, Nano Energy 104 (2022), 107940, https://doi.org/10.1016/j.nanoen.2022.107940.
[34] L. Da Via, C. Recchi, T.E. Davies, N. Greeves, J.A. Lopez-Sanchez, Visible-light-controlled oxidation of glucose using titania-supported silver photocatalysts, ChemCatChem 8 (2016) 3475–3483, https://doi.org/10.1002/cctc.201600775.
[35] S. Hao, H. Zhang, X. Sun, J. Zhai, S. Dong, A mediator-free self-powered glucose biosensor based on a hybrid glucose/MnO_2 enzymatic biofuel cell, Nano Res 14 (2021) 707–714, https://doi.org/10.1007/s12274-020-3101-5.
[36] A.J. Gross, M. Holzinger, S. Cosnier, Buckypaper bioelectrodes: emerging materials for implantable and wearable biofuel cells, Energy Environ. Sci. 11 (2018) 1670–1687, https://doi.org/10.1039/c8ee00330k.
[37] W. Wu, Q. Wang, J. Chen, L. Huang, H. Zhang, K. Rong, S. Dong, Biomimetic design for enhancing the peroxidase mimicking activity of hemin, Nanoscale 11 (2019) 12603–12609, https://doi.org/10.1039/c9nr03506k.
[38] L. Gao, X. Yan, Nanozymes: an emerging field bridging nanotechnology and biology, Sci. China.: Life Sci. 59 (2016) 400–402, https://doi.org/10.1007/s11427-016-5044-3.
[39] L. Zhang, H. Cui, Z. Zou, T.M. Garakani, C. Novoa-Henriquez, B. Jooyeh, U. Schwaneberg, Directed evolution of a bacterial laccase (CueO) for enzymatic biofuel cells, Angew. Chem., Int. Ed. 58 (2019) 4562–4565, https://doi.org/10.1002/anie.201814069.
[40] L. Xu, J. Chen, Q. Ma, D. Chao, X. Zhu, L. Liu, J. Wang, Y. Fang, S. Dong, Critical evaluation of the glucose oxidase-like activity of gold nanoparticles stabilized by different polymers, Nano Res 16 (2023) 4758–4766, https://doi.org/10.1007/s12274-022-5218-1.
[41] W.J. Luo, C.F. Zhu, S. Su, D. Li, Y. He, Q. Huang, C.H. Fan, Self-catalyzed, self-limiting growth of glucose oxidase-mimicking gold nanoparticles, ACS Nano 4 (2010) 7451–7458, https://doi.org/10.1021/nn102592h.
[42] X. Niu, M. Wang, H. Zhu, P. Liu, J. Pan, B. Liu, Nanozyme catalysis-assisted ratiometric multicolor sensing of heparin based on target-specific electrostatic-induced aggregation, Talanta 238 (2022), 123003, https://doi.org/10.1016/j.talanta.2021.123003.